

FRM4SST Project: Measurement Uncertainty Budgets











www.ships4sst.org June 2025

Document Ref: FRM4SST-MUB-SCL-002 Customer : ESA

Contract No : 3-15990/19/NL/IA Issue Date : 14 July 2025 WP No : 50 Issue : Issue 1

Reference : FRM4SST-MUB-SCL-002

Title FRM4SST Project: Measurement Uncertainty Budgets

This document contains a description of the measurement uncertainty budgets used by **Abstract**

the FRM4SST project team during the year 2024 - 2025.

Author

Approved

Werenfrid Wimmer, UoS (Technical Leader)

Ruth Wilson, Sorrel Nelson, SCL Werenfrid Wimmer, UoS

Tim Nightingale, RAL

Accepted by ESA:

Craig Donlon ESA Technical Officer

Distribution: FRM4SST Project Team

ESA

EUROPEAN SPACE AGENCY CONTRACT REPORT

The work described in this document was done under ESA contract. Responsibility for the contents resides in the author or organisation that prepared it.









Document Version Control

Issue	Revision	Date of issue	Description of changes
		/ revision	
Draft	A (Version	26/02/2025	Updated document for the year 2023- 2024 with
	2)		draft new section created (version 2)
Draft	В	14/07/2025	Details of the SISTeR model added by Tim
			Nightingale and final internal review
Issue	1	14/07/2025	Document issued to ESA









TABLE OF CONTENTS

1.	EX	(ECUTIVE SUMMARY	
		TRODUCTION	
		Overview	
		THE ISAR MODEL	
		THE SISTER MODEL	
3.	UN	NCERTAINTY RESULTS	16
4.	UN	NCERTAINTY VALIDATION	21
5.	MO	ODEL UPDATES	24
6.	СО	ONCLUSION	29
		CRONYMS AND ABBREVIATIONS	
		FERENCES	31









LIST OF FIGURES AND TABLES

for an external view......

Figure 2-1: T	he ISAR SST Measurements equation featuring a breakdown of some of the main elements of the ISAR SST processor to show the factors that introduce uncertainties. The boxes coloured in blue represent Type A uncertainties, boxes coloured in red show Type B uncertainties, and boxes in red and blue contain both Type A and Type B uncertainties. R2T stands for radiation to temperature transformation, R _{sea} is the radiation from the sea, R _{sky} the radiation from the sky, ε the seawater emissivity, R _{BB1,2} the radiation from the two on-board blackbodies, and Sig _{Sea} , Sig _{Sky} , Sig _{BB1,2} are the signal from the detector when viewing the sea, sky of the two blackbodies (<u>Wimmer and Robinson, 2016</u>)
Figure 2-2: S	ources of uncertainties arising within the ISAR SST retrieval processor11
Figure 2-3 T	he SISTeR Level 2 equation, showing the breakdown of calculation elements. Individual terms are summarised in Table 2-1. The Level 1 equation is identical, with the exception that the synthetic count c* is replaced by the detector count









Figure 4-2: The	e ISAR 03 – ISAR 12 inter-comparison on the James Clark Ross. The left panel shows the ISAR 03 uncertainty versus the SST _{skin} difference of SISTeR – ISAR, and the right panel shows the ISAR 12 uncertainty versus the SST _{skin} difference of SISTeR – ISAR. The red dot shows the median with the standard errors as error bars, the blue shows the standard deviation, the magenta dot shows the mean and the green lines are the theoretical limit
Figure 4-3: ISA	R 03 – ISAR 07 inter-comparison on the Discovery. The left panel shows the ISAR 03 uncertainty versus the SST_{skin} difference of SISTeR – ISAR , and the right panel shows the ISAR 07 uncertainty versus the SST_{skin} difference of SISTeR – ISAR. The red dot shows the median with the standard errors as error bars, the blue shows the standard deviation, the magenta dot shows the mean and the green lines are the theoretical limit.
Figure 5-1: The	e plot shows ISAR uncertainty model version 1 with SST _{skin} against time and the colour representing the total uncertainty24
Figure 5-2:The	plot shows ISAR uncertainty model version 2 with SST _{skin} against time and the colour representing the total uncertainty
Figure 5-3: The	e plot shows ISAR uncertainty model version 3 with SST _{skin} against time and the colour representing the total uncertainty25
Figure 5-4: SIS	TeR – ISAR inter-comparison on the Queen Mary 2. The left top panel shows the SISTeR uncertainty versus the SST _{skin} difference of SISTeR – ISAR, the left bottom panel shows the ISAR uncertainty version 1 versus the SST _{skin} difference of SISTeR – ISAR, the right top panel shows the ISAR uncertainty version 2 versus the SST _{skin} difference of SISTeR – ISAR, and the right bottom panel shows the ISAR uncertainty version 3 versus the SST _{skin} difference of SISTeR – ISAR. The red dot shows the median with the standard errors as error bars, the blue shows the standard deviation, the magenta dot shows the mean and the green lines are the theoretical limit.
Figure 5-5: ISA	AR 03 – ISAR 12 inter-comparison on the James Clark Ross. The left top panel shows the ISAR 12 uncertainty versus the SST _{skin} difference of ISAR 03 – ISAR 12, the left bottom panel shows the ISAR 03 uncertainty version 1 versus the SST _{skin} difference of ISAR 03 – ISAR 12, the right top panel shows the ISAR 03 uncertainty version 2 versus the SST _{skin} difference of ISAR 03 – ISAR 12, and the right bottom panel shows the ISAR 03 uncertainty version 3 versus the SST _{skin} difference of ISAR 03 – ISAR 12. The red dot shows the median with the standard errors as error bars, the blue shows the standard deviation, the magenta dot shows the mean and the green lines are the theoretical limit
Figure 5-6: ISA	AR 03 – ISAR 07 inter-comparison on the James Clark Ross. The left top panel shows the ISAR 07 uncertainty versus the SST _{skin} difference of ISAR 03 – ISAR 07, the left bottom panel shows the ISAR 03 uncertainty version 1 versus the SST _{skin} difference of ISAR 03 – ISAR 07, the right top panel shows the ISAR 03 uncertainty version 2 versus the SST _{skin} difference of ISAR 03 – ISAR 07, and the right bottom panel shows the ISAR 03 uncertainty version 3 versus the SST _{skin} difference of ISAR 03 – ISAR 07. The red dot shows the median with the standard errors as error bars, the blue shows the standard deviation, the magenta dot shows the mean and the green lines are the theoretical limit









EXECUTIVE SUMMARY

The FRM4SST project is funded by the European Space Agency (ESA) and, through various activities, aims to sustain and evolve the International Sea Surface Temperature (SST) Fiducial Reference Measurement (FRM) Network (ISFRN). One way that this aim is fulfilled is through the collection, processing, analysis, publication and reporting of *in situ* FRM field measurements made using ISAR and SISTeR Instruments, that are near-contemporaneous with satellite data from the Sentinel-3A and Sentinel-3B SLSTR instruments.

The objectives for the FRM4SST project are:

- OBJ-1: Deploy and maintain shipborne thermal infrared (TIR) FRM radiometers and necessary supporting instrumentation to validate satellite SST products.
- OBJ-2: Maintain FRM protocols for satellite SST measurements and uncertainty budgets.
- OBJ-3: Process, quality control, archive and deliver approved FRM4SST data sets following documented FRM procedures and approve their use for FRM satellite validation.
- OBJ-4: Validate satellite SST products to FRM standards and publish monthly results.
- OBJ-5: Promote the FRM4SST outputs and maintain the International SST FRM Radiometer Network (ISFRN).

In order to ensure that the SLSTR geophysical data products are reliable, the *in situ* data that the products are validated against need to have a reliable uncertainty budget associated with them (OBJ-2).

This report is deliverable D3 on the FRM4SST contract and describes the uncertainty budgets used by the FRM4SST Team. The FRM4SST uncertainty budgets for shipborne radiometers and supporting measurements used for satellite SST validation will continue to be updated and maintained through the project lifetime.









2. INTRODUCTION

2.1 Overview

For satellite-derived SST datasets to be used for the compilation of climate data records (CDRs) in which SST is regarded as an essential climate variable (ECV) (Bojinski et al. 2014), a rigorous approach to satellite data quality should be followed, as recommended by Barker et al. (2015). Most notably, this implies that the *in situ* SST observations used for validating satellite datasets should be accompanied with estimates of the uncertainty of each SST record, in accordance with formal metrological protocols (JCGM 2008) that are now incorporated into the Committee on Earth Observation Satellites (CEOS) specifications for CDRs (QA4EO Task Team 2010). More recently, these independent ground-based SST measurements are labelled as Fiducial Reference Measurements (FRM). Donlon et.al 2014 defines the mandatory characteristics for FRM as:

- 1. FRM measurements have documented evidence of SI traceability via inter-comparison of instruments under operational-like conditions.
- 2. FRM measurements are independent from the satellite SST retrieval process.
- 3. An uncertainty budget for all FRM instruments and derived measurements is available and maintained, traceable where appropriate to SI ideally directly through an NMI.
- 4. FRM measurement protocols and community-wide management practices (measurement, processing, archive, documents, etc.) are defined and adhered to.

All of the above points are addressed by the FRM4SST project, point 1 is satisfied by regular inter-comparisons, the last one being conducted in 2022 (see Yamada, Y., et.al. 2024 and 2024a). The second point is addressed by the careful design of the shipborne radiometers such as ISAR, SISTeR and M-AERI (Donlon et.al 2008, Minnet et.al. 2001) and their processing system (Wimmer et.al. 2016). The third point will be discussed in this report and the final point is addressed by the FRM4SST project in publishing the community wide protocol and measurement strategies on the ships4sst website.

A comprehensive and reliable uncertainty budget allows a dataset to be compared either with themselves or with a reference standard and as such, can be used with confidence. Uncertainties arise due to many reasons but can be grouped into the following primary categories (Donlon et al. 2014a¹) as:

¹ https://doi.org/10.1016/B978-0-12-417011-7.00018-0









- **Instrument measurement uncertainty**: those relating to instrument hardware e.g. detector noise, optical misalignment, etc.
- Retrieval/algorithm uncertainty: those relating to derived quantities e.g. the value of sea water emissivity, temporal differences between sea surface and atmospheric radiance measurements, etc.
- Application uncertainty: those relating to a specific application e.g. differences in the type of SST measurement (e.g. of SST_{depth} or SST_{skin}).

These uncertainties can further be split into two categories as described by **Donlon et al. 2014**.:

- Measurement uncertainty: The uncertainty associated with the typical variability of the measured property, e.g., variability of the brightness temperature (BT) of the sea and sky view measurements, or the uncertainty of seawater emissivity, etc.
- Instrument uncertainty: The uncertainty related to the instrument introduces regardless of the measured property such as detector noise, thermistor calibrations, electronics digitization uncertainty, and so on.

Another way of evaluating uncertainties is according to the character of the uncertainty, which broadly maps to the more commonly used terms of systematic and random uncertainties, where Type A uncertainties are often labelled as random uncertainties and Type B uncertainties as systematic uncertainties. Wimmer and Robinson, 2016, describe Type A and Type B uncertainties as:

- Type A: Uncertainties that must be estimated by using statistics, sometimes also referred to as random, since the uncertainties can be reduced by increasing the number of samples used in producing a single data record.
- Type B: Uncertainties estimated from knowledge of component behaviour or other information, sometimes also referred to as systematic, because they are not reduced by obtaining more samples.

As an example of such a shipborne uncertainty model, we look at the ISAR uncertainty model as described by Wimmer et.at. 2016. The ISAR model uses Type A and Type B uncertainties, which mainly include above Instrument measurement uncertainty and Retrieval/algorithm uncertainty. A more thorough investigation into how these categories relate specifically to shipborne radiometer SST measurements can be found in Donlon et al. 2014.









2.2 The ISAR Model

A comprehensive uncertainty budget and analysis for a shipborne radiometer has been produced by Wimmer et al. 2012 and Wimmer and Robinson, 2016 for the ISAR radiometer. The ISAR uncertainty model was created based on FRM standards and requirements and so not only are pre- and post-deployment calibrations performed but also a per-measurement model is used. This means that not only are shipborne radiometers fully traceable to SI standards (Preston-Thomas et al. 1990) but it also reduces the need for a large number of nominally independent observations to reduce the random uncertainty (for example, in the case of drifting buoys). The ISAR uncertainty model is based on a breakdown of uncertainties for the entire end-to-end instrument and data processing system, and was developed on a first principle bases by analysing these components of the ISAR instrument and propagating their associated uncertainties through the measurement equation that is shown in Figure 2-1 (Wimmer and Robinson, 2016). Type A uncertainties are coloured in blue and Type B uncertainties are coloured in red. Boxes with both colours indicate that the component contains both Type A and Type B uncertainties.

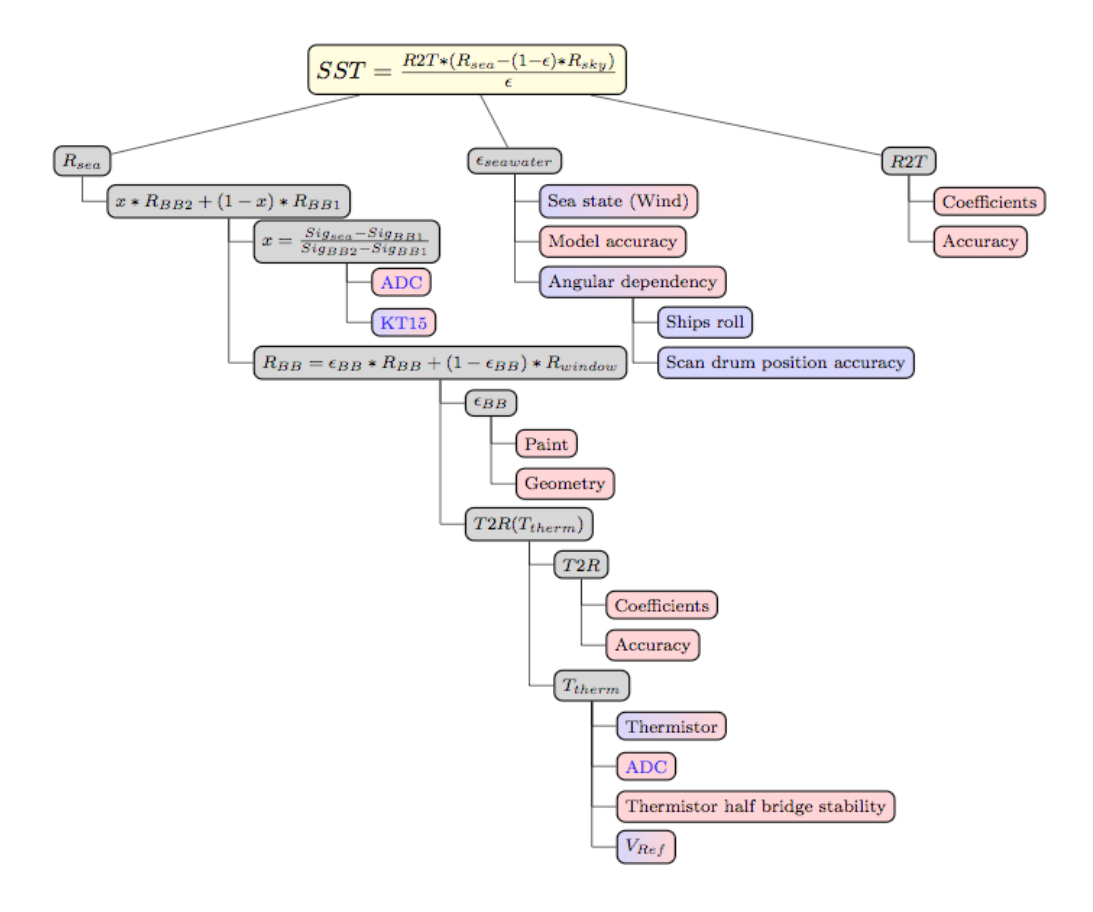


Figure 2-1: The ISAR SST Measurements equation featuring a breakdown of some of the main elements of the ISAR SST processor to show the factors that introduce uncertainties. The boxes coloured in blue represent Type A uncertainties, boxes coloured in red show Type B uncertainties, and boxes in red and blue contain both Type A and Type B uncertainties. R2T stands for radiation to temperature transformation, R_{sea} is the radiation from the sea, R_{sky} the









radiation from the sky, ϵ the seawater emissivity, $R_{BB1,2}$ the radiation from the two on-board blackbodies, and Sig_{Sea} , Sig_{Sky} , $Sig_{BB1,2}$ are the signal from the detector when viewing the sea, sky of the two blackbodies (Wimmer and Robinson, 2016).

Figure 2-2 shows the main sources of uncertainty for the ISAR instrument, an indication of it values and range and if it is a Type A or Type B uncertainty. Wimmer and Robinson, 2016, discuss every item on the list in Figure 2-2 extensively, with justifications and supporting literature.

e	Item	Uncertainty	Unit	Type
1	Detector linearity	< 0.01%	K month ⁻¹	В
2	Detector noise	~0.002	Volts	A
3	Detector accuracy	±0.5	K	В
4	ADC	$\pm 1(\pm 76.3)$	LSB (μV)	В
5	ADC accuracy	±0.1%	Range	В
6	ADC zero drift	±6	$\mu V \circ C^{-1}$	В
7	Reference voltage 16-bit ADC	±15	mV	В
8	Reference voltage 12-bit ADC	±20	mV	В
9	Reference resistor	1	%	В
10	Reference resistor temperature coefficient	±100	Ppm °C ^{−1}	В
11	BB emissivity	± 0.000178	Emissivity	В
12	Sea surface emissivity	±0.07	Emissivity	В
13	Steinhart-Hart approximation	±0.01	K	В
14	Radiate transfer approximation	± 0.001	K	В
15	Thermistor	±0.05	K	В
16	Thermistor noise	~0.002	V	A

Figure 2-2: Sources of uncertainties arising within the ISAR SST retrieval processor.

Wimmer and Robinson, 2016, also provide some simple uncertainty propagation models to study the sensitivity of the ISAR SST processor to verify the steps needed in the uncertainty estimation for a self-calibrating radiometer such as ISAR and concluded on the following approach:

- 1. The thermistors' uncertainties are calculated by first assigning the ADC uncertainty to the measured voltage. The resistance of the thermistor is then calculated by taking the uncertainty of the reference voltage and the reference resistor into account. The resistance is converted into a temperature by using the Steinhart–Hart approximation, taking the uncertainty of the approximation into account. The uncertainty resulting from this temperature calculation is then combined with the manufacturer-quoted thermistor uncertainty of 60.05 K and the variability of the thermistor temperature during a blackbody (BB) target view to derive the thermistor uncertainty used in the temperature-to-radiance transformation.
- For the detector signal, the ADC uncertainty and the detector temperature dependence, using
 the temperature of the detector case thermistor (which is calculated using the approach
 described above) and the variability over each target view, are used to calculate the detector
 signal uncertainty.









- 3. The internal BB radiances with uncertainties are then calculated using the BB and window thermistor temperatures together with the internal BB emissivity uncertainty.
- 4. Now the sky view and sea view radiances can be calculated by first calibrating the detector signal together with its uncertainties, and then using the calibrated detector signal to calculate sky and sea radiances with the associated uncertainty from the BB radiances. The BB radiances are estimated as described in step 1.
- 5. The sea water emissivity is estimated using the Niclòs et al., 2009, model averaged over a wind speed range of 0 - 20 m/s with the view angle calculated from the maximum ship roll during the sea view and sky view.
- 6. The penultimate step is calculating the SST with a total uncertainty by using the sea and sky radiances and their associated uncertainties together with the sea water emissivity and its uncertainty.
- 7. The final step is to add the CASOTS II BB uncertainty (Donlon et al., 2014) in quadrature to the uncertainty, as calculated by the previous steps. This step is necessary only because of the different responses of the half-bridge resistor circuit of individual ISARs. Without this step, the traceability is achieved through the BB thermistors.

The Type A uncertainties are estimated in the averaging calculation at each of the BB views and the sea view and sky view. The averaging at each of these views is necessary to reduce the detector noise.

2.3 The SISTeR Model

The SISTeR Level 2 processor implements the retrieval equation:

$$SSB = \frac{L_{sea} - \rho' L_{sky}}{1 - \rho'} - k b_{air}$$

Where SSB is the sea surface Planck radiance associated with a perfectly black source at the sea surface temperature, L_{sea} and L_{sky} are the upwelling sea radiance and the complementary downwelling sky radiance at the instrument aperture, ρ' is the sea surface reflectance, modified by the transmittance of the optical path from the instrument to the sea surface and b_{air} is the air radiance anomaly with respect to the sea surface radiance. The SSB term appears on both sides of the equation, but as the air temperature typically is not measured directly and is usually close to the sea surface temperature, the anomaly can be approximated to be zero (with a suitable uncertainty).

As the sea and sky radiances share calibration information from the two internal black bodies, BB1 and BB2, it can be shown that the retrieval equation is equivalent to a direct calibration of a synthetic count







 c^* derived from the signal counts c_{sea} and c_{sky} recorded while observing the sea and sky respectively (Figure 2-3). This approach avoids "double counting" of the calibration uncertainties that would result if the sea and sky radiances are derived independently.

The processor is broken down into functional elements following the calculation elements in Figure 2-1. Each function accepts a value for each input term, along with an estimate of its random and systematic uncertainties (as variances), calculates the core function and its partial derivatives and returns an output value with estimates of its random and systematic uncertainties (again as variances).

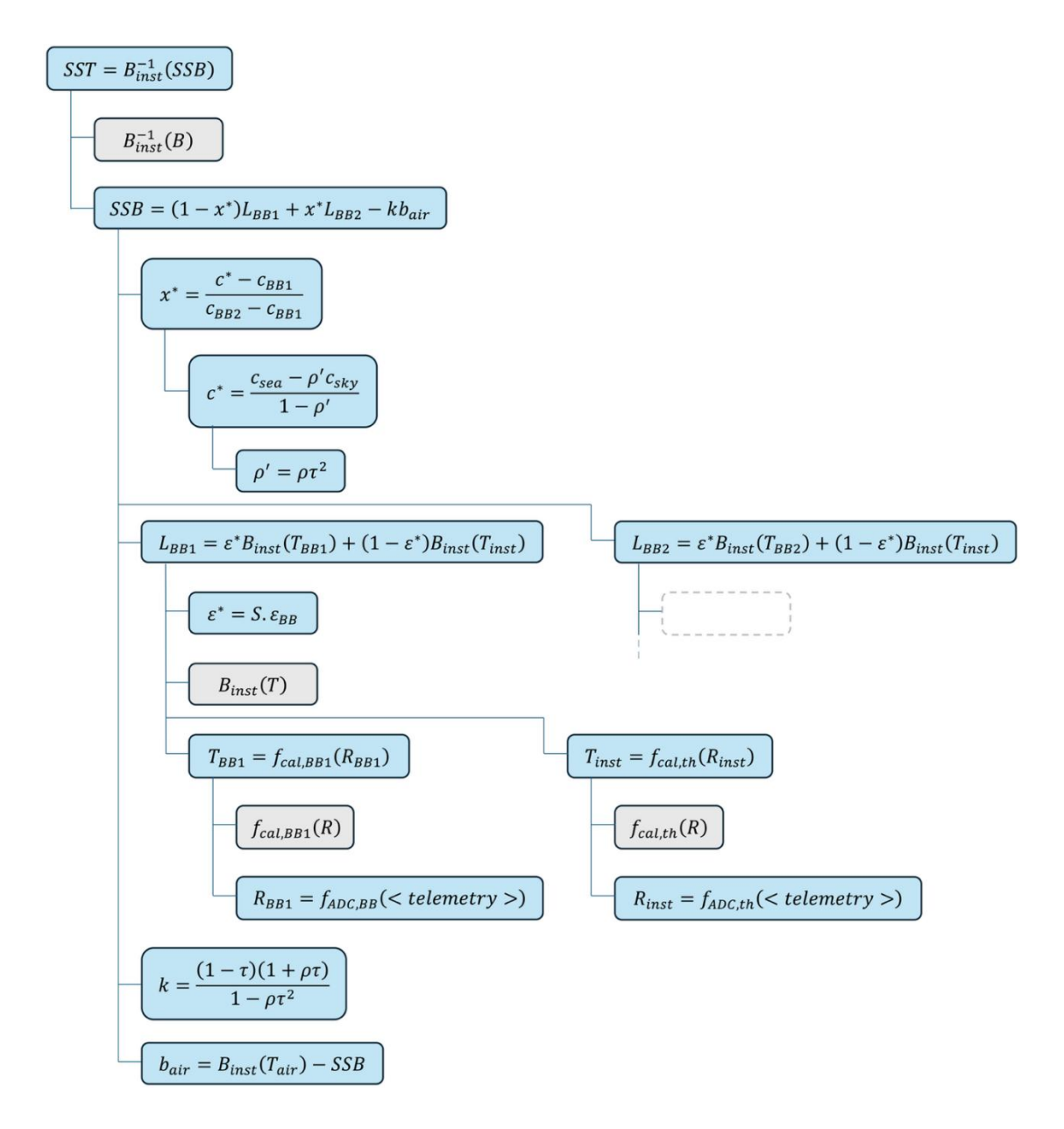


Figure 2-3 The SISTeR Level 2 equation, showing the breakdown of calculation elements. Individual terms are summarised in Table 2-1. The Level 1 equation is identical, with the exception that the synthetic count c^* is replaced by the detector count for an external view.









Table 2-1 Summary of terms used in the SISTeR Level 2 equation

	-
SST	Sea surface skin temperature
SSB	Planck radiance associated with the SST, weighted by the instrument spectral response function (ISRF)
L_{BB1}, L_{BB2}	Black body radiances
$B_{inst}(T), B_{inst}^{-1}(B)$	Planck function weighted by the ISRF, and its inverse
<i>x</i> *	Proportional position of SBB between the two black body radiances
<i>c</i> *	Synthetic detector count corresponding to SSB
C_{BB1}, C_{BB2}	Detector counts for measurements of BB1 and BB2
c_{sea}, c_{sky}	Detector counts for measurements of the sea surface and sky
ρ'	Modified sea surface reflectance
ρ	Sea surface reflectance, weighted by the ISRF
τ	Air transmittance weighted by the ISRF for the slant path from the sea surface to the instrument
$arepsilon^*$	Effective black body emissivity
\mathcal{E}_{BB}	Black body emissivity weighted by the ISRF
S	Size-of-source and vignetting correction
T_{BB1} , T_{BB2}	Black body temperatures
$f_{cal,BB1}(R), f_{cal,BB2}(R)$	Black body traceable thermometer calibration functions
R_{BB1}, R_{BB2}	Black body thermometer impedances
$f_{ADC,BB}(< telemetry >)$	Black body thermometer bridge transfer function
T_{inst}	Instrument temperature
$f_{cal,th}(R)$	Housekeeping thermistor calibration function
R _{inst}	Housekeeping thermistor impedance
$f_{ADC,th}(< telemetry >)$	thermistor bridge transfer function
k	Air radiance anomaly sensitivity
b_{air}	Air radiance anomaly

Random uncertainties are determined where possible from the instrument telemetry. Detector noise, for instance, is estimated from the variances of the black body observations. Systematic uncertainties, calibration parameters and configuration information are stored in a hierarchy of XML auxiliary files which follow the deployment platform, instrument and major instrument subsystems. Each file is split into a "history" of validity time intervals. The correct parameters are found by walking the hierarchy tree to identify the instrument installed on the platform at the measurement time, the subsystems installed in the instrument and the valid calibration parameters for the subsystem.

All instrument telemetry is interpolated onto the detector sample timestep (800 ms). As the thermometry telemetry is slowly varying, it is interpolated with a one-dimensional Kalman smoother. Black body and sky view detector counts are multiplexed in time with the sea view measurements and so are propagated to the detector sample times by linear interpolation between averages of the black body and sky views. The random sky view observation uncertainty is estimated as the RMS difference of a









step change in the sky signal at the halfway point from the linear trend, in other words, the quantisation noise, or $(c_{skv,i+1} - c_{skv,i})/\sqrt{12}$.

For the filter in use, the dependence of instrument Planck radiance on temperature is modelled by a modified Planck function:

$$B_{inst}(T) = \frac{a_0}{exp\left(\sum_{i=0}^{n} \frac{a_{i+1}}{T^i}\right) - 1}$$

This is both differentiable and easily invertible for expressions that are up to quadratic (n = 2) in 1/T, and can reproduce scene radiances with an equivalent fitting error of a few µK. For internal calculations, a_0 is chosen so that $B_{inst}(273.15 \text{ K}) = 1$, and so that consequently the magnitudes of derived radiance values are always reasonable. The actual value is unimportant, so long as it is used consistently. This is guaranteed as all Planck radiance-related calculations ($B_{inst}(T),\ B_{inst}^{-1}(B),\ \frac{dB_{inst}}{dT}$) use the same coefficient set.









3. UNCERTAINTY RESULTS

The ISAR uncertainty model produces a number of outputs including the total uncertainty, the instrument and measurement uncertainty, and the Type A and Type B uncertainties for each SSTskin data point as shown in Figure 3-1 and Figure 3-2. Furthermore, a number of uncertainties dependences plots are produced to be able to monitor the performance of the ISAR uncertainty model which are shown in Figure 3-3 and Figure 3-4.

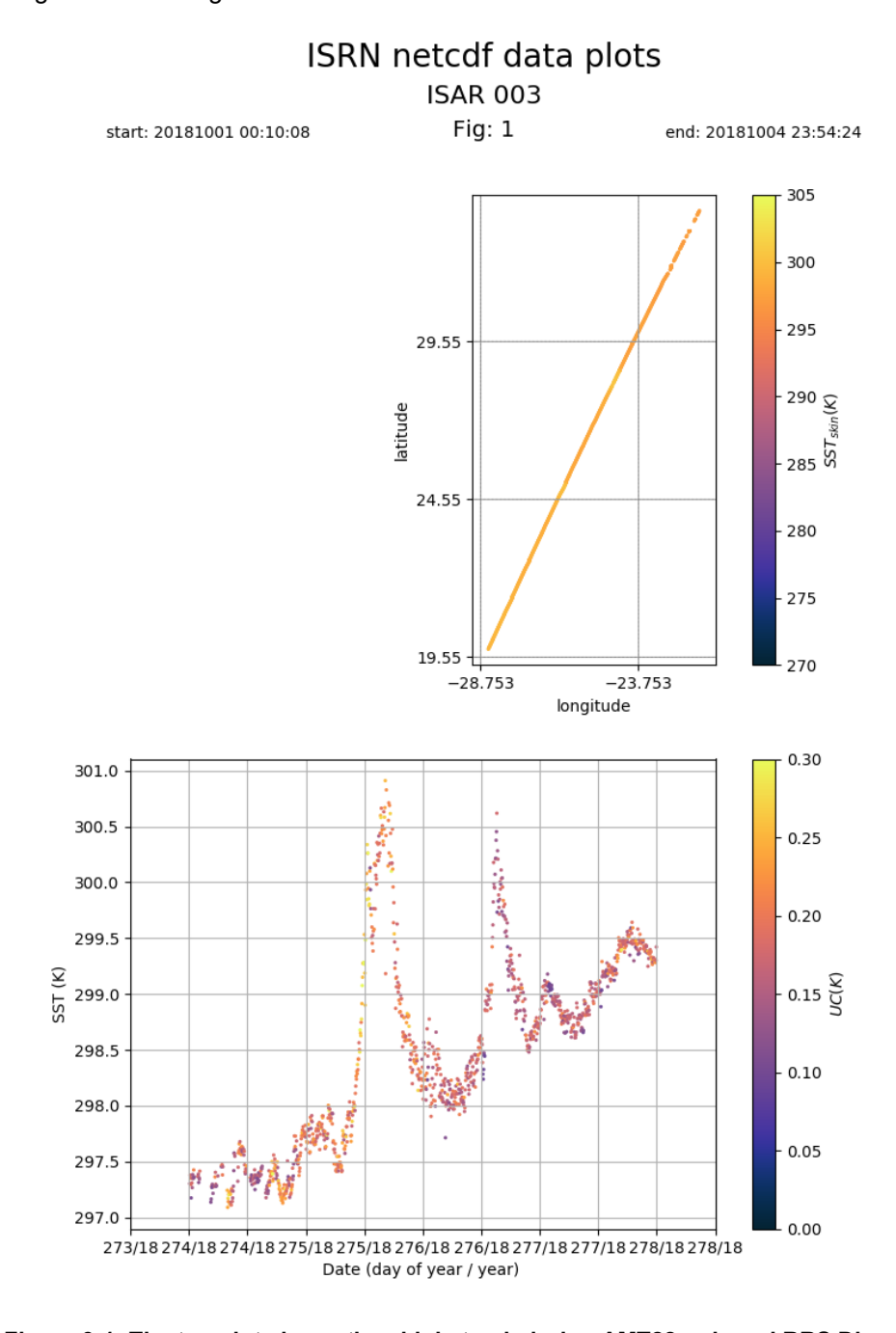


Figure 3-1: The top plot shows the ship's track during AMT28 onboard RRS Discovery fieldwork in October 2018, with the colour of the track representing the measured SSTskin. The bottom plot shows the SSTskin over time with the colour representing the uncertainty as calculated by the ISAR uncertainty model.









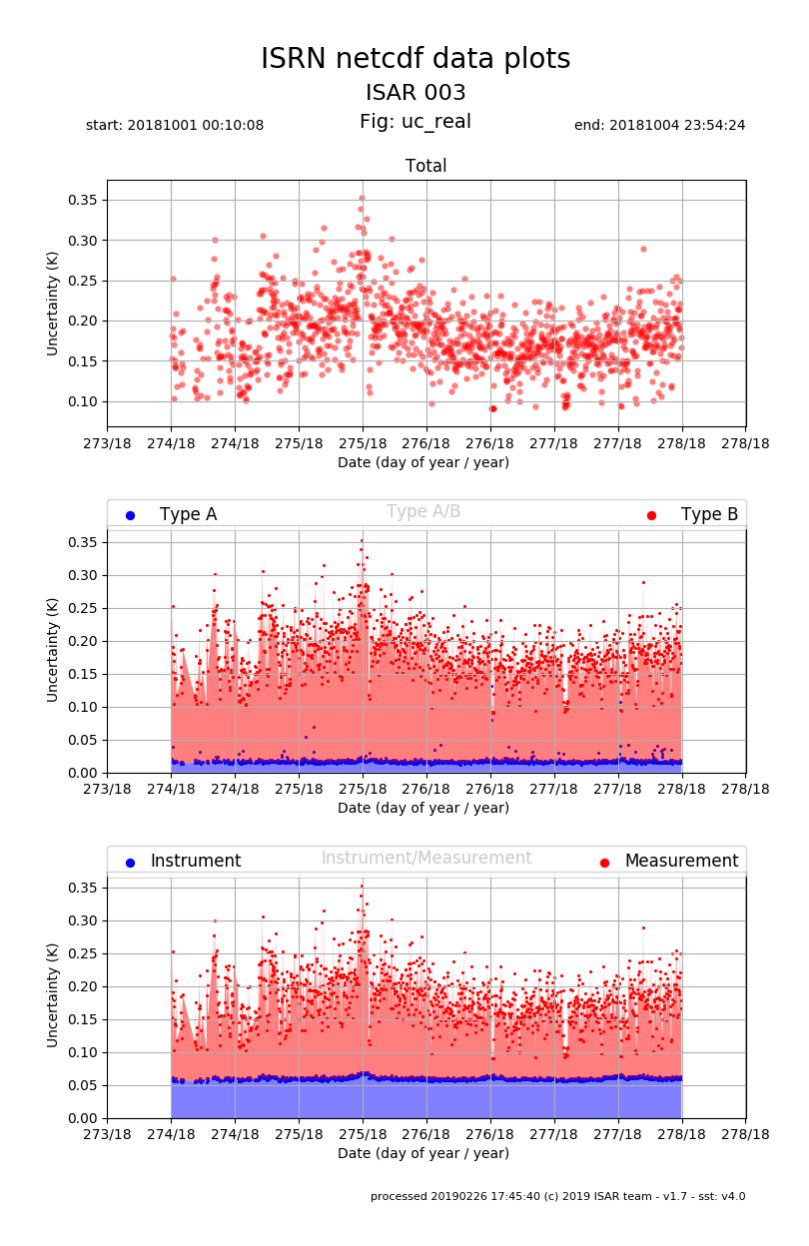


Figure 3-2: The top panel shows the total ISAR uncertainty over time, the middle panel shows the total ISAR uncertainty split into Type A (blue) and Type B (red) uncertainty, and the bottom panel shows the total ISAR uncertainty split into instrument (blue) and measurement uncertainty.

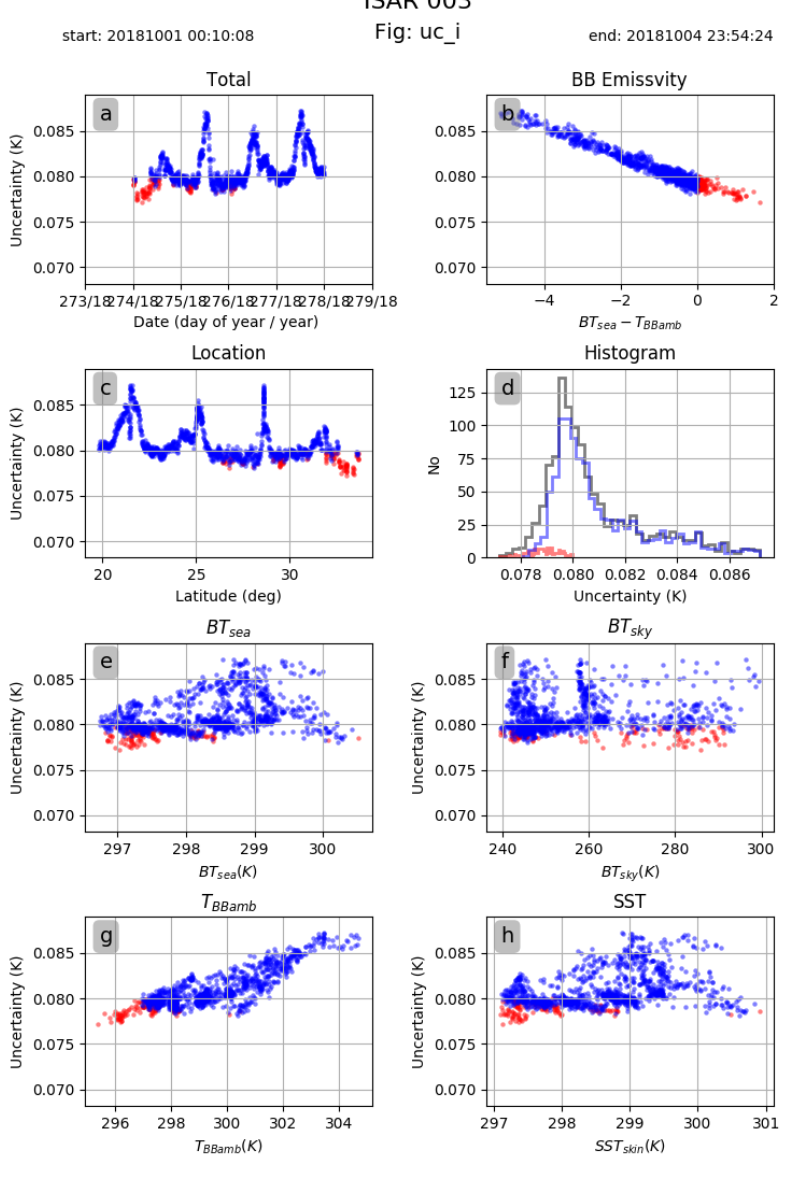








ISRN netcdf data plots ISAR 003



processed 20190226 17:45:37 (c) 2019 ISAR team - v1.7 - sst: v4.0

Figure 3-3: The figure shows ISAR instrument uncertainty versus a number of parameters: Panel a shows the total uncertainty, panel b shows the uncertainty in over the BT_{sea} – T_{BBamb} difference, panel c shows the uncertainty plotted against the latitude and panel d shows a histogram of the uncertainty. Panel e shows the uncertainty plotted against the BT_{sea}, panel f shows the uncertainty plotted against the BT_{sky}, panel g shows the uncertainty plotted against the temperature of the ambient BB, and panel h shows the uncertainty plotted against the SST_{skin}. The blue dots represent data where BT_{sea} is colder than the ambient BB and red dots show data where BT_{sea} is between the ambient BB and the hot BB.









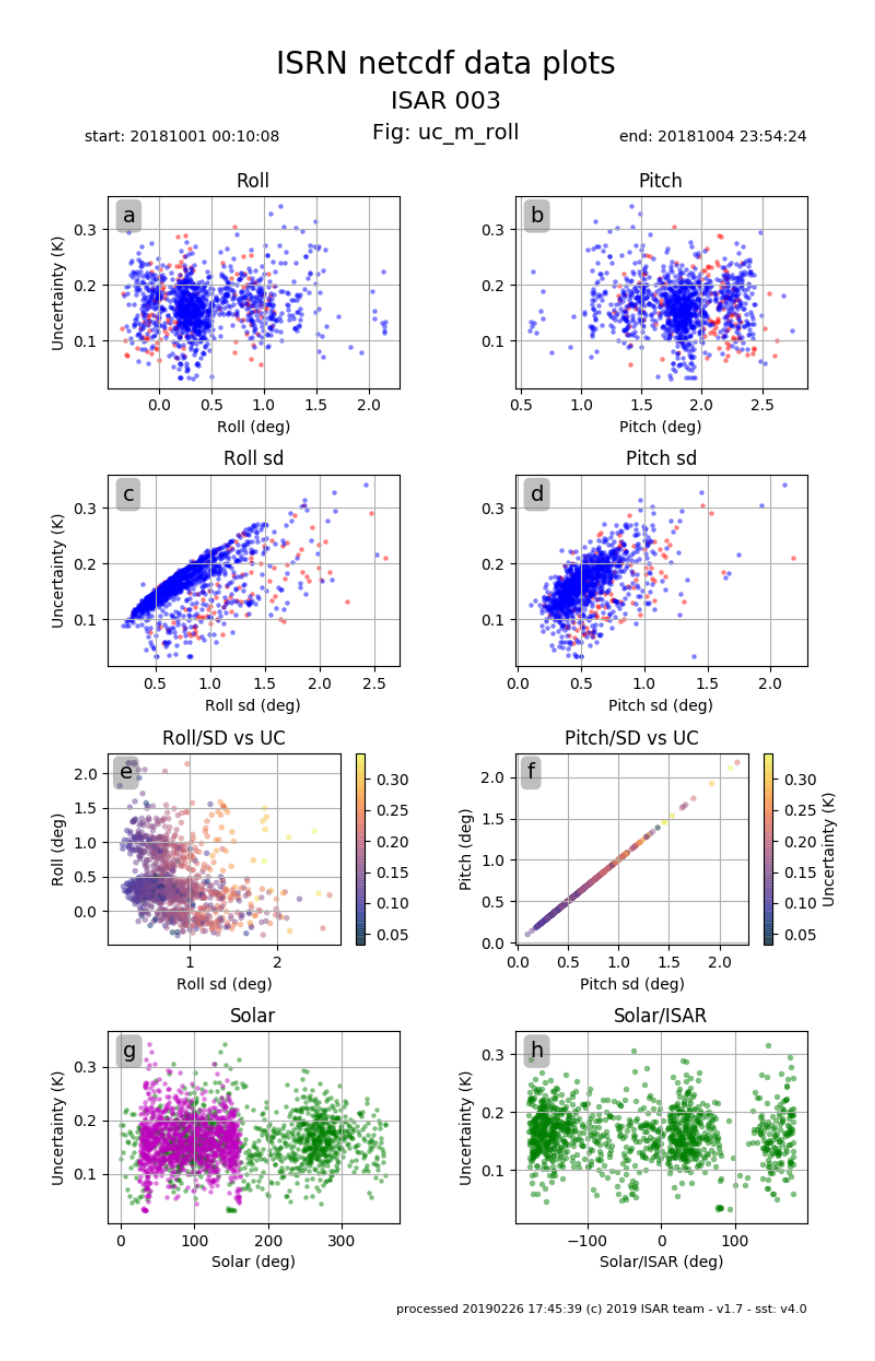


Figure 3-4: The plots show the measurement uncertainties dependence versus a number of parameters: Panel a shows the uncertainty to roll relationship, panel b shows the uncertainty to pitch relationship, panel c shows the uncertainty to the standard deviation of the roll during one scan cycle, panel c shows the uncertainty to the standard deviation of the pitch during one scan cycle, panel e shows roll versus the rolls standard deviation with the colour representing the uncertainty, panel f shows pitch versus the pitch standard deviation with the colour representing the uncertainty, panel g shows the uncertainty vs the suns azimuth (green) and zenith angle (purple), and panel h shows the uncertainty versus the solar azimuth angle relative to ISAR.









Overall, the approach by Wimmer and Robinson, 2016, for a shipborne radiometer uncertainty model seem to work very well, however, important considerations to address include the following, as stated by Donlon, 2014:

- · Are all significant terms included in the instrument and measurement uncertainty budget?
- How should one handle the large uncertainty associated with broken cloud conditions that result
 in a differently measured sky radiance compared to the sky radiance at the time of sweater
 radiance measurement (i.e. a cloud is present in one measurement but not the other), Donlon
 and Nightingale, 2000?
- What is the best way to determine a geophysical component for the natural SST_{skin} variability that is expected to be more variable than the SST_{subskin} or SST_{depth} (Donlon et.al., 2005)?
- Most importantly, there is a need to validate the uncertainty estimates for all shipborne TIR
 FRM radiometers. The next section will try and address this point.







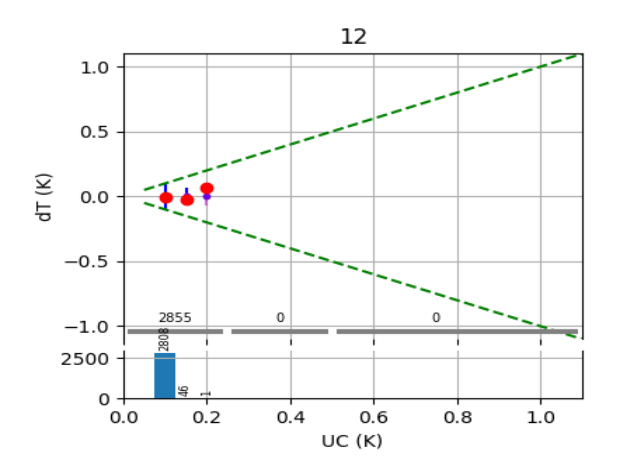


4. UNCERTAINTY VALIDATION

Uncertainty validation is a key requirement and essential for the user's confidence in those uncertainties. The overall performance of the shipborne radiometers have been verified through regular inter-comparisons, starting in 1999, 2001, 2009, 2016, and the most recent one in 2022 (see Yamada 2024, 2024a) showing that they perform to their stated uncertainty in laboratory and semi controlled filed conditions such as a pier. However, because shipborne radiometers are expensive and ship time even more so, there have not been many at sea inter-comparison of shipborne radiometers. Nevertheless, a number of at sea comparisons have been carried out to verify the ISAR uncertainty model over the years, such as:

- SISTeR ISAR 03, M/V Queen Mary 2, 18.10.2015 to 05.11.2015
- ISAR 03 ISAR 12, RRS James Clark Ross, 24.09.2018 to 29.10.2018
- ISAR 03 ISAR 07, RRS Discovery, 12.10.2019 22.11.2019

These side-by-side comparisons were used to verify the ISAR uncertainty model and to check if any parameters produce inconsistent results.



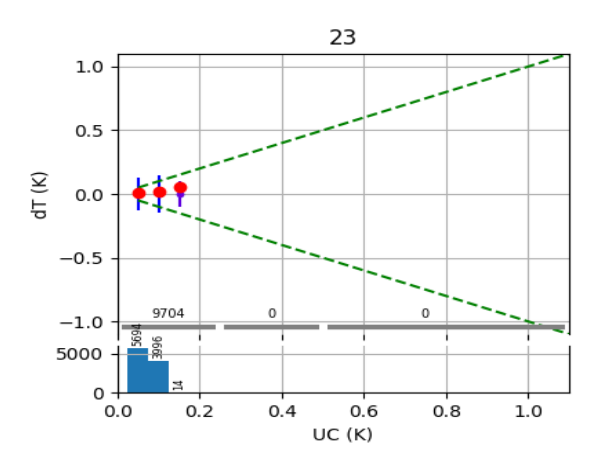


Figure 4-1: SISTER – ISAR inter-comparison on the Queen Mary 2. The left panel shows the SISTER uncertainty versus the SST_{skin} difference of SISTER – ISAR, and the right panel shows the ISAR uncertainty versus the SST_{skin} difference of SISTER – ISAR. The red dot shows the median with the standard errors as error bars, the blue shows the standard deviation, the magenta dot shows the mean and the green lines are the theoretical limit.

The SISTeR – ISAR at sea comparison showed that both instruments performed very similarly and the uncertainty model works very well for small uncertainties.









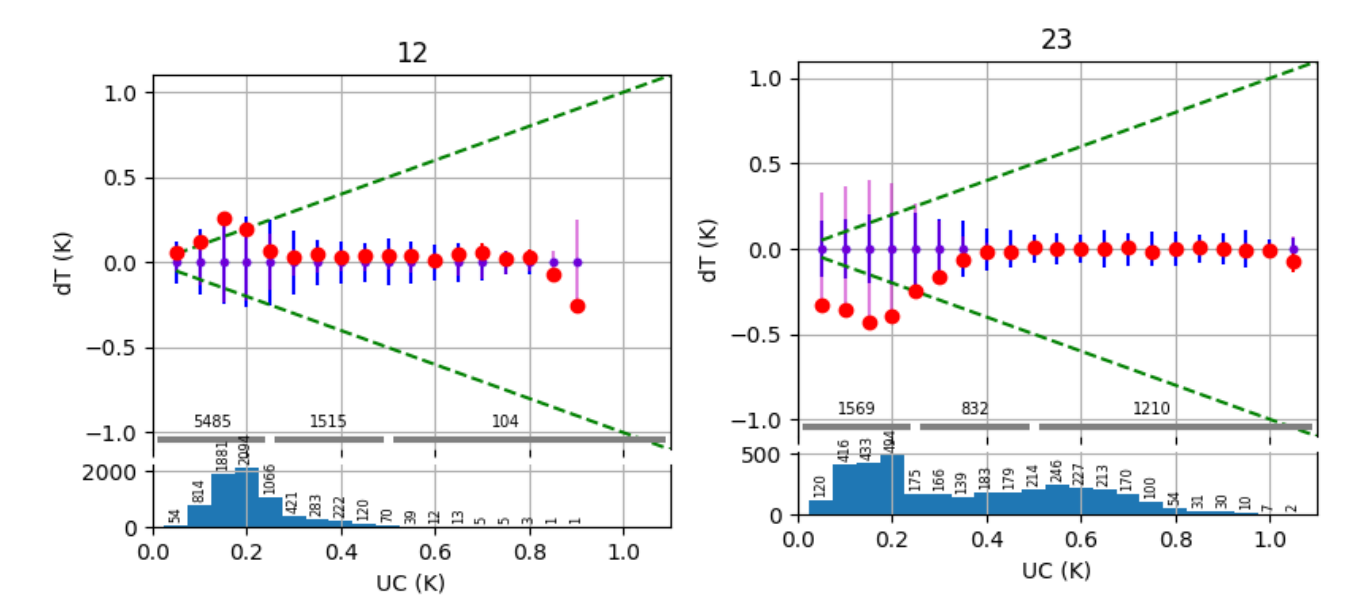


Figure 4-2: The ISAR 03 – ISAR 12 inter-comparison on the James Clark Ross. The left panel shows the ISAR 03 uncertainty versus the SST_{skin} difference of SISTeR – ISAR, and the right panel shows the ISAR 12 uncertainty versus the SST_{skin} difference of SISTeR – ISAR. The red dot shows the median with the standard errors as error bars, the blue shows the standard deviation, the magenta dot shows the mean and the green lines are the theoretical limit.

The ISAR 03 to ISAR 12 inter-comparison showed again a good agreement at low uncertainties, but also showed the overestimation of uncertainties which is due to a high sensitivity of the emissivity on the roll of the ship. It also showed an issue with ISAR 12 during the deployment, resulting in the large low uncertainties compared to ISAR 03.









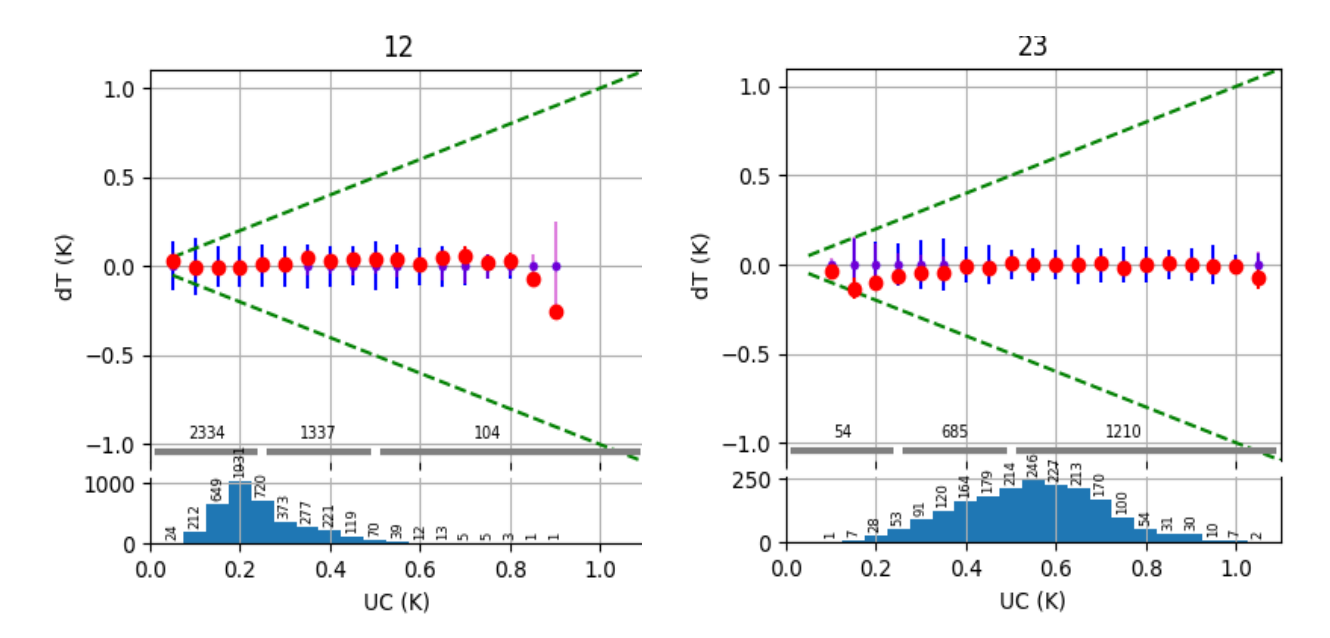


Figure 4-3: ISAR 03 – ISAR 07 inter-comparison on the Discovery. The left panel shows the ISAR 03 uncertainty versus the SST_{skin} difference of SISTeR – ISAR, and the right panel shows the ISAR 07 uncertainty versus the SST_{skin} difference of SISTeR – ISAR. The red dot shows the median with the standard errors as error bars, the blue shows the standard deviation, the magenta dot shows the mean and the green lines are the theoretical limit.

The ISAR 03 to ISAR 07 inter-comparison showed again a good agreement at low uncertainties, and confirmed what was seen on the comparison on the James Clark Ross; an overestimation of uncertainties due to a high sensitivity of the emissivity on the roll of the ship.









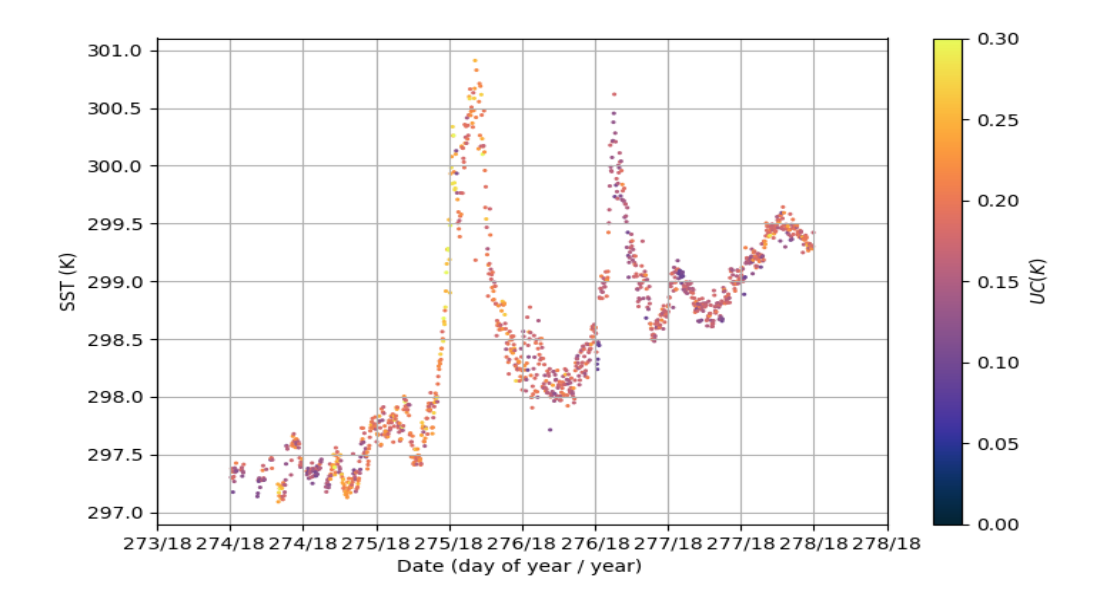
5. MODEL UPDATES

The ISAR uncertainty validation showed an over-estimation of high uncertainties, which is due to the emissivity roll dependence model used. To reduce the roll dependence of the sea water emissivity, a number of changes were introduced for version 2 compared to the ISAR uncertainty model version 1:

- Roll is Hanning filtered, length is 11 values
- Sky and sea signals use over 5 SST samples
 - Centre Weighted average is 1, 4, 4,1
 - Variance of the signal gets added to the sea and sky signal uncertainty before internal calibration

And in order to get some idea of the geophysical induced uncertainty, a geophysical indicator was introduced for version 3:

• SST weighted std gets estimated as geophysical indicator → extra uncertainty variable



processed 20190226 17:45:31 (c) 2019 ISAR team - v1.7 - sst: v4.0

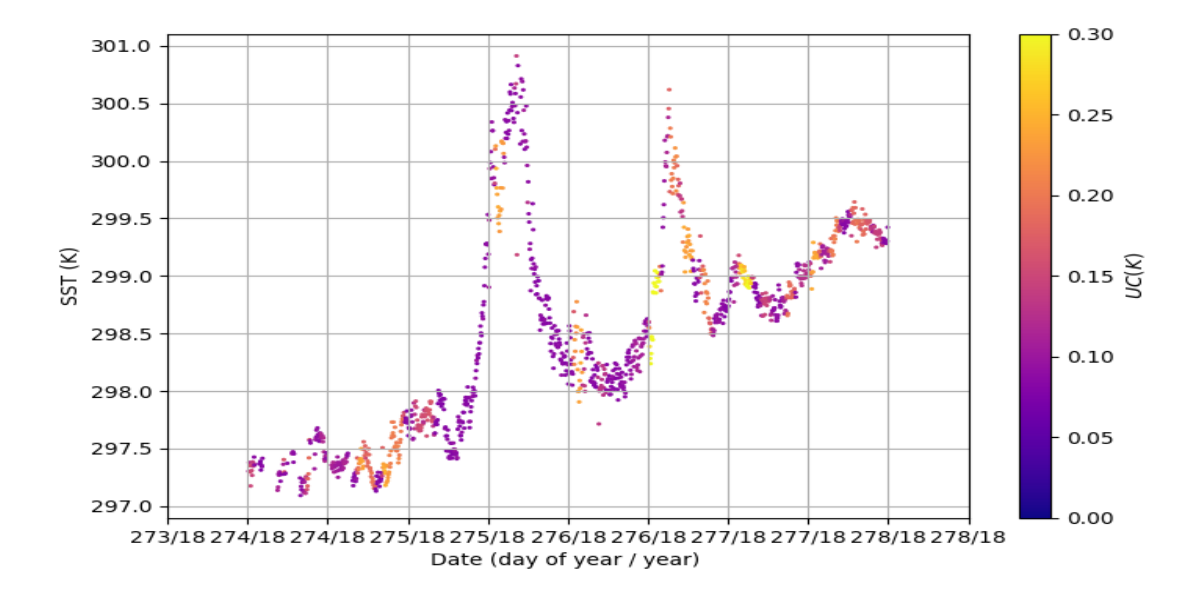
Figure 5-1: The plot shows ISAR uncertainty model version 1 with SST_{skin} against time and the colour representing the total uncertainty.





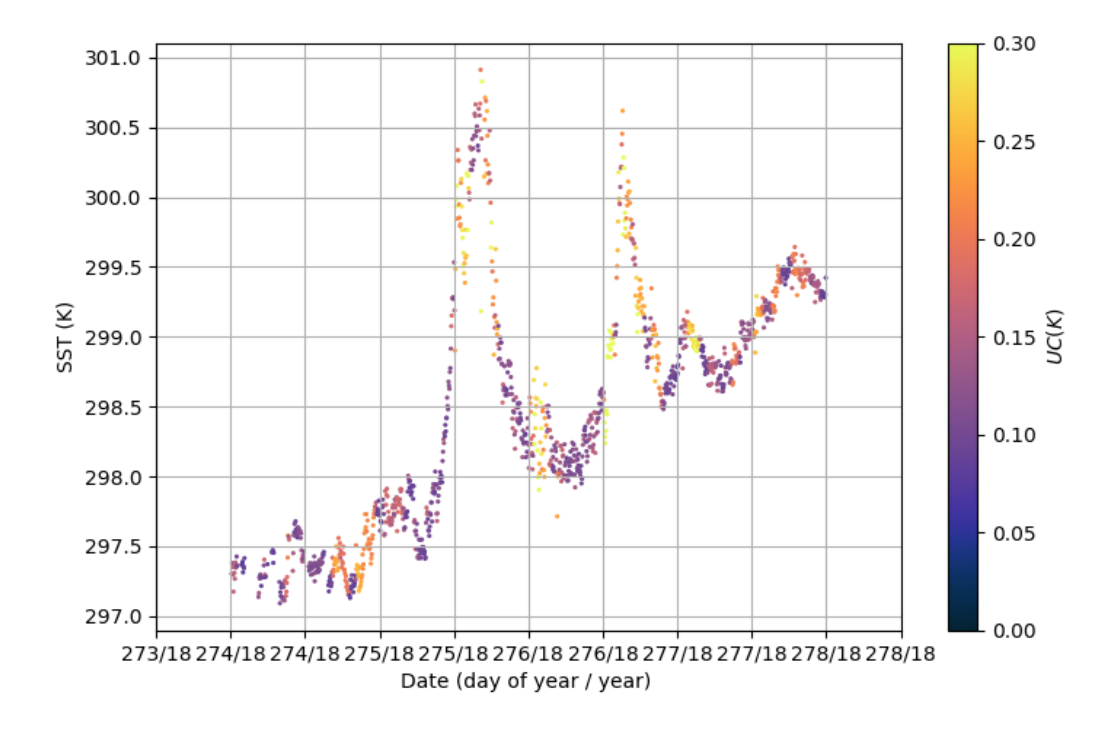






processed 20210520 19:20:21 (c) 2021 ISAR team - v1.7 - sst: v4.4

Figure 5-2:The plot shows ISAR uncertainty model version 2 with SST_{skin} against time and the colour representing the total uncertainty.



processed 20190226 18:09:15 (c) 2019 ISAR team - v1.0 - sst: v 4.1

Figure 5-3: The plot shows ISAR uncertainty model version 3 with SST_{skin} against time and the colour representing the total uncertainty.









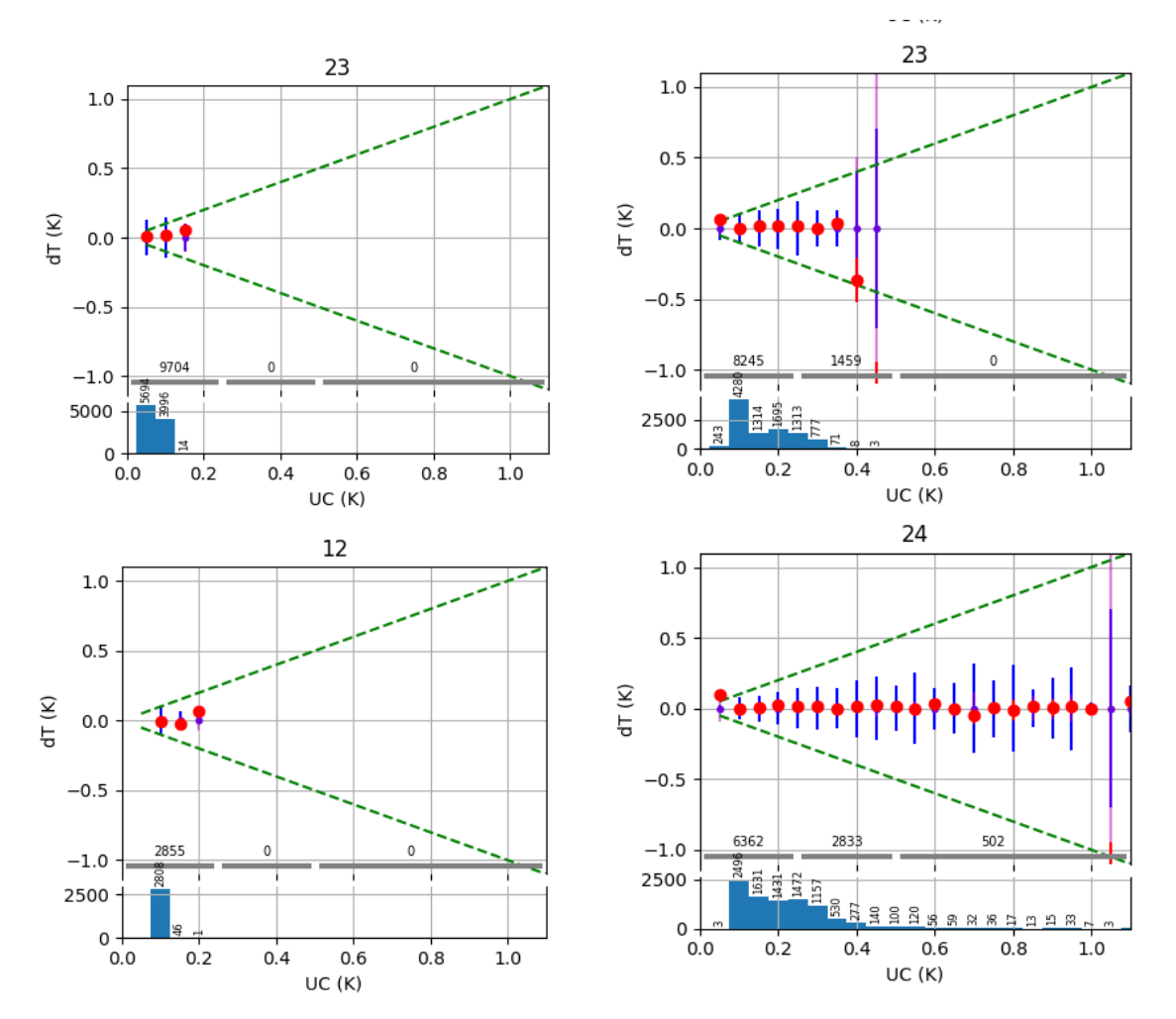


Figure 5-4: SISTeR – ISAR inter-comparison on the Queen Mary 2. The left top panel shows the SISTeR uncertainty versus the SST_{skin} difference of SISTeR – ISAR, the left bottom panel shows the ISAR uncertainty version 1 versus the SST_{skin} difference of SISTeR – ISAR, the right top panel shows the ISAR uncertainty version 2 versus the SST_{skin} difference of SISTeR – ISAR, and the right bottom panel shows the ISAR uncertainty version 3 versus the SST_{skin} difference of SISTeR – ISAR. The red dot shows the median with the standard errors as error bars, the blue shows the standard deviation, the magenta dot shows the mean and the green lines are the theoretical limit.









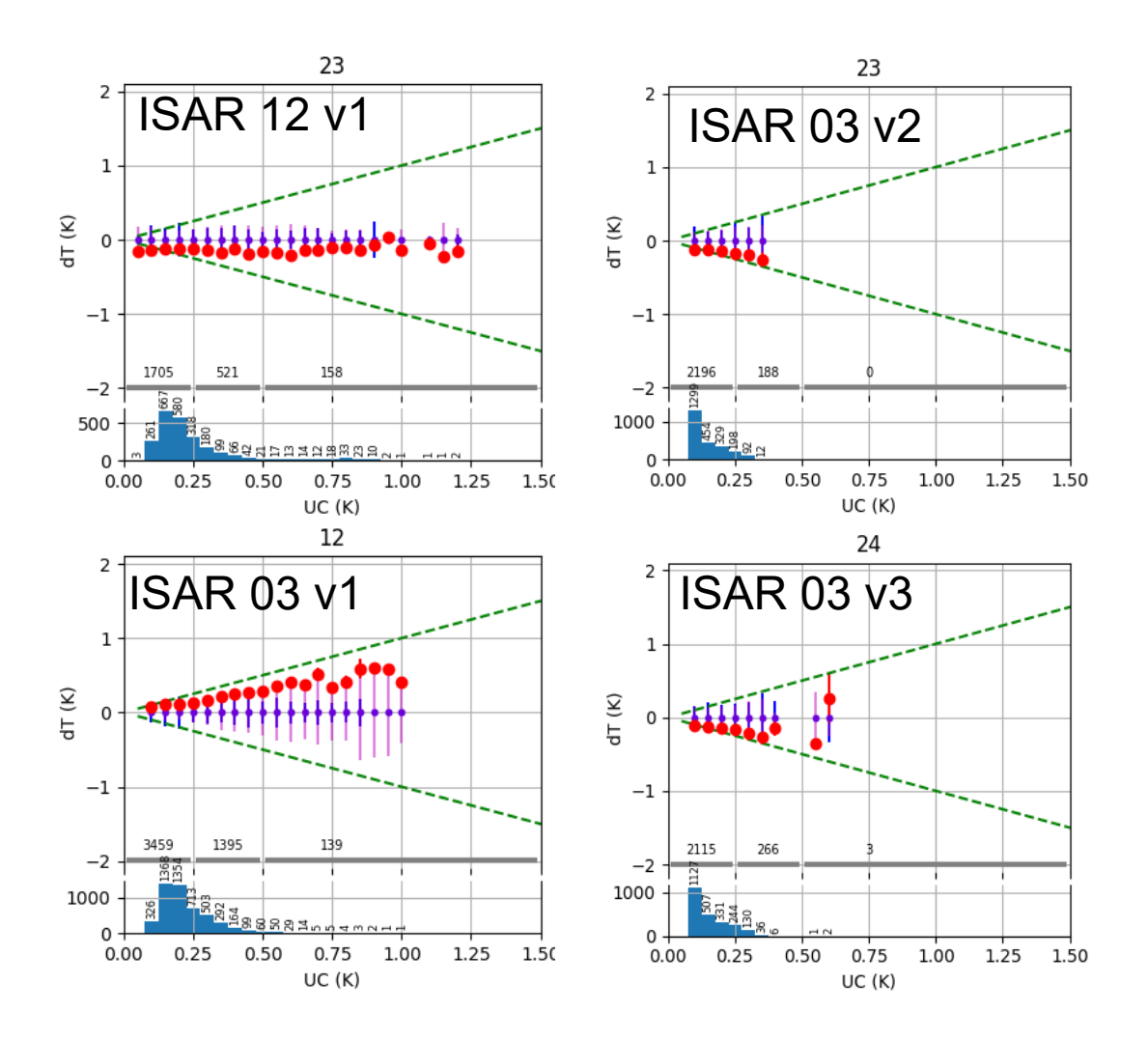


Figure 5-5: ISAR 03 – ISAR 12 inter-comparison on the James Clark Ross. The left top panel shows the ISAR 12 uncertainty versus the SST_{skin} difference of ISAR 03 – ISAR 12, the left bottom panel shows the ISAR 03 uncertainty version 1 versus the SST_{skin} difference of ISAR 03 – ISAR 12, the right top panel shows the ISAR 03 uncertainty version 2 versus the SST_{skin} difference of ISAR 03 – ISAR 12, and the right bottom panel shows the ISAR 03 uncertainty version 3 versus the SST_{skin} difference of ISAR 03 – ISAR 12. The red dot shows the median with the standard errors as error bars, the blue shows the standard deviation, the magenta dot shows the mean and the green lines are the theoretical limit.







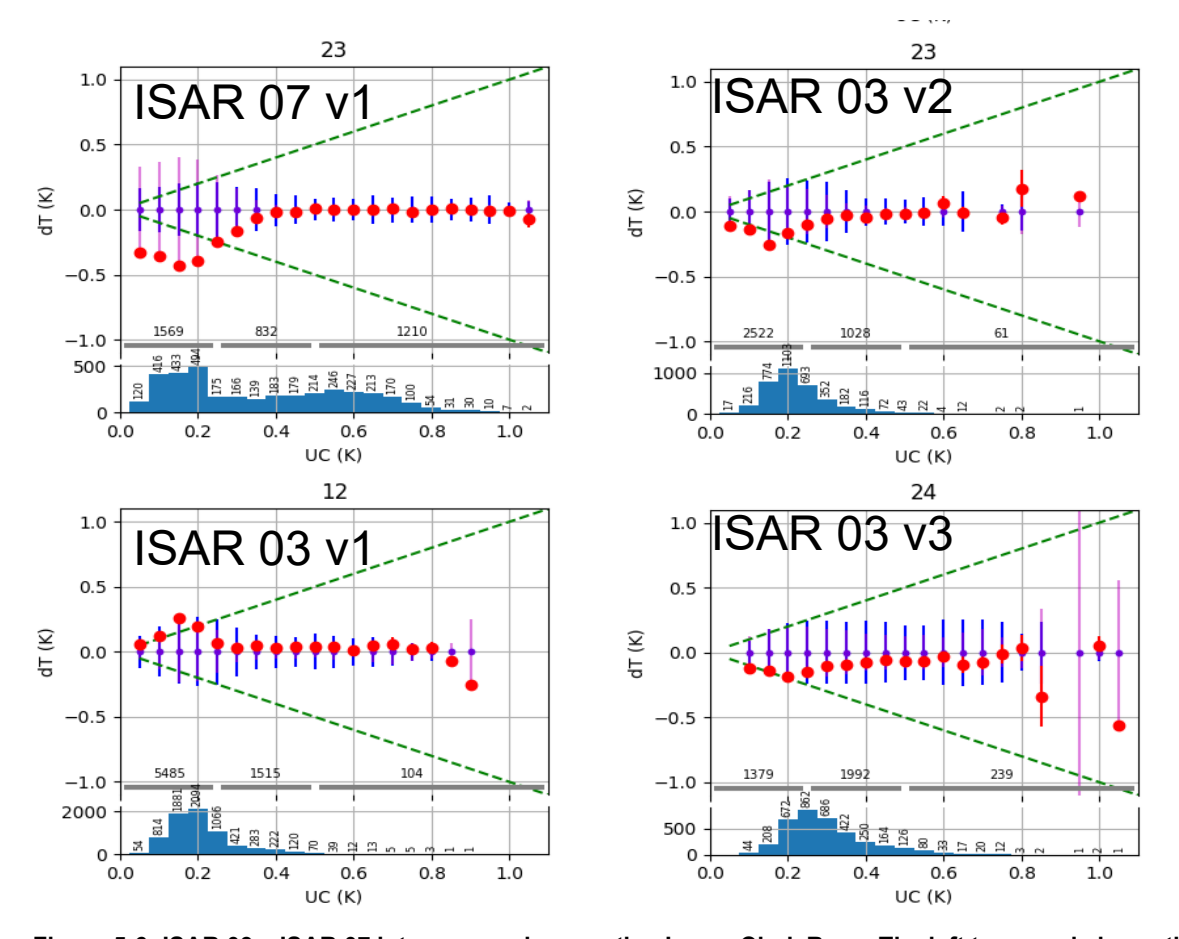


Figure 5-6: ISAR 03 – ISAR 07 inter-comparison on the James Clark Ross. The left top panel shows the ISAR 07 uncertainty versus the SST_{skin} difference of ISAR 03 – ISAR 07, the left bottom panel shows the ISAR 03 uncertainty version 1 versus the SST_{skin} difference of ISAR 03 – ISAR 07, the right top panel shows the ISAR 03 uncertainty version 2 versus the SST_{skin} difference of ISAR 03 – ISAR 07, and the right bottom panel shows the ISAR 03 uncertainty version 3 versus the SST_{skin} difference of ISAR 03 – ISAR 07. The red dot shows the median with the standard errors as error bars, the blue shows the standard deviation, the magenta dot shows the mean and the green lines are the theoretical limit.

The data from the comparison shows that the new ISAR uncertainty model addresses the roll dependence issue of the emissivity, however, while version 2 and version 3 seem to be an improvement over version 1, more work is needed as its clear from the data that there are either misrepresented or unresolved cross-correlation issue in the model.









6. CONCLUSION

It is essential for climate data records to have a verifiable uncertainty model. In order for satellites to be able to be seen as a CDR they need validation data which not only is traceable but also has a verifiable uncertainty model, especially if the ground data wants to be recognised as an FRM. The ISAR and SISTeR uncertainty models are an example of a shipborne radiometer FRM uncertainty model that is derived from first principle, and performs excellently under controlled conditions. However, more work is needed to understand the measurements uncertainty in the field better.

The validation of the FRM uncertainty models is essential but non trivial, and the datasets are sparse, especially at the higher uncertainties. Furthermore, investigating the areas where the uncertainty models are currently under-performing is not a simple task and will require not only man power but also funding.









7. ACRONYMS AND ABBREVIATIONS

AATSR Advanced Along-Track Scanning Radiometer

ATSR Along-Track Scanning Radiometer

BB Blackbody

CDR Climate Data Record

Essential Climate Variable ECV

EDS Engineering Data System

ΕO Earth Observation

ESA European Space Agency

EU **European Union**

FRM Fiducial Reference Measurements

FRM4STS Fiducial Reference Measurements for validation of Surface

Temperature from Satellites

GHRSST Group for High Resolution SST

IR Infra-Red

ISAR Infrared SST Autonomous Radiometer

ISFRN International SST FRM Radiometer Network

LST Land Surface Temperature

M-AERI Marine-Atmospheric Emitted Radiance Interferometer

NOCS National Oceanography Centre, Southampton

RAL Rutherford Appleton Laboratory

RSD Robust Standard Deviation

SCL Space ConneXions Limited

SISTeR Scanning Infrared Sea surface Temperature Radiometer

SLSTR Sea and Land Surface Temperature Radiometer

SST Sea Surface Temperature

ST Surface Temperature

STFC Science and Technology Facilities Council

TIR Thermal Infra-Red









8. REFERENCES

The recommended ISFRN L2R Data Specification and User Manual, T. Nightingale, ships4sst.

Werenfrid Wimmer, Ian S. Robinson, Craig J. Donlon, Long-term validation of AATSR SST data products using shipborne radiometry in the Bay of Biscay and English Channel, Remote Sensing of Environment, Volume 116, 2012, Pages 17-31, ISSN 0034-4257, https://www.sciencedirect.com/science/article/abs/pii/S0034425711002094?via%3Dihub/

Wimmer, W. & Robinson, I. S. The ISAR Instrument Uncertainty Model, Journal of Atmospheric and Oceanic Technology, 2016, 33, 2415-2433

Theocharous, E.; Fox, N. P.; Barker-Snook, I.; Niclòs, R.; Garcia Santos, V.; Minnett, P. J.; Göttsche, F. M.; Poutier, L.; Morgan, N.; Nightingale, T.; Wimmer, W.; Høyer, J.; Zhang, K.; Yang, M.; Guan, L.; Arbelo, M. & Donlon, C. J. The 2016 CEOS infrared radiometer comparison: Part 2: Laboratory comparison of radiation thermometers. Journal of Atmospheric and Oceanic Technology, 2018.

Yamada, Y., and Coauthors, 2024; 2022 CEOS International Thermal Infrared Radiometer Comparison. Part I: Laboratory Comparison of Radiometers and Blackbodies. J. Atmos. Oceanic Technol., 41, 295-307, https://doi.org/10.1175/JTECH-D-23-0059.1.

Yamada, Y., and Coauthors, 2024a: 2022 CEOS International Thermal Infrared Radiometer Comparison. Part II: Field Comparison of Radiometers. J. Atmos. Oceanic Technol., 41, 309-318, https://doi.org/10.1175/JTECH-D-23-0060.1.

Craig J. Donlon, Peter J. Minnett, Nigel Fox, Werenfrid Wimmer, Chapter 5.2 - Strategies for the Laboratory and Field Deployment of Ship-Borne Fiducial Reference Thermal Infrared Radiometers in Support of Satellite-Derived Sea Surface Temperature Climate Data Records, Editor(s): Giuseppe Zibordi, Craig J. Donlon, Albert C. Parr, Experimental Methods in the Physical Sciences, Academic Press, Volume 47, 2014, Pages 557-603, ISBN 9780124170117, https://doi.org/10.10<u>16/B978-0-12-417011-7.00018-0</u>.

Barker, A., A. Banks, W. Bell, M. Dowell, N. P. Fox, P. Green, and M. Whitney, 2015: Metrology for climate: Metrology priorities for the earth observation and climate community. A. Barker et al., Eds., National Physics Laboratory Tech. Rep., 36 pp. [Available online at https://eprintspublications.npl.co.uk/6728/1/metrology for climate report.pdf

Minnett, P.; Knuteson, R.; Best, F.; Osborne, B.; Hanafin, J. & Brown, O. The Marine-Atmospheric Emitted Radiance Interferometer: A High-Accuracy, Seagoing Infrared Spectroradiometer. J. Atmos. Oceanic Technol., 2001, 18, 994-1013

Donlon, C.; Robinson, I.; Reynolds, M.; Wimmer, W.; Fisher, G.; Edwards, R. & Nightingale, T. An Infrared Sea Surface Temperature Autonomous Radiometer (ISAR) for Deployment aboard Volunteer Observing Ships (VOS) J. Atmos. Oceanic Technol., 2008, 25, 93-113

C.J. Donlon, T.J. Nightingale, The effect of atmospheric radiance errors in radiometric sea surface temperature measurements, Appl. Opt. 39 (2000) 2392e2397.

C.J. Donlon, W. Wimmer, I.S. Robinson, G. Fisher, D. Poulter, G. Corlett, Validation of AATSR using in situ radiometers in the English channel and Bay of Biscay, in: ESA MERIS602 Optical Radiometry for Ocean Climate Measurements and (A)ATSR Workshop 2005, ESRIN Frascati, Italy, ESA-SP-597. ISSN: 1609-042X, 2005, ISBN 92-9092-908-1. Available

online:https://www.researchgate.net/publication/234283059 Validation of AATSR Using In Situ Radiometers in the English Channel and Bay of Biscay





